

MECHANISMS OF INTERFACIAL LOCOMOTION IN THE INDIAN SKIPPER FROG

Author: Talia Weiss^a

Collaborators: Sanjay Sane^b, Michelle Graham^a, Sunghwan Jung^c,
Ty Hedrick^d & Jake Socha^a (advisor)

^aDept. of Biomedical Engineering And Mechanics, Virginia Tech, Blacksburg VA

^bNational Centre for Biological Sciences, Bangalore, India

^cDept. of Biological and Environmental Engineering, Cornell, Ithaca NY

^dDept. of Biology, UNC, Chapel Hill NC

Abstract

The Indian skipper frog, *Euphlyctis cyanophlyctis*, can skitter, or jump on the water surface without sinking. However, this behavior has never been examined in detail. The goal of this study is to quantitatively describe the characteristics of skittering by analyzing high speed video recordings of the frogs performing this behavior in the wild. We recorded a total of 109 skittering events, 60 of which were filmed with at least 2 synced cameras to allow for 3D calibration. We found that during a skittering event a frog on average jumps about 3 times after launching from water, but are capable of jumping up to 9. To date we have reconstructed 27 trajectories of the frog's interfacial locomotion in 3D. From these reconstructions, we found that these frogs are fairly maneuverable while skittering, often turning during this behavior. Additionally, the frogs travel on average 25 cm in 132 ms for each jump. Once additional kinematics parameters are calculated, we will be able to use them to physically model what happens when the frog's foot hits the water so that we can begin to probe the physics involved in skittering.

Introduction

A large, phylogenetically diverse number of animals exhibit some form of interfacial locomotion – movement that occurs on or through the air-water interface⁵. Most of these animals are small and lightweight, able to statically support themselves solely through

surface tension. However, there are a few animals that are able to move across the water surface despite their large size and weight. Because they are too heavy to be supported by surface tension, these animals have to move, taking advantage of inertial effects to dynamically support themselves on the water surface. While inertial water-walkers that use a running-like gait have been studied previously in the basilisk lizard^{13,14,17,18} and grebe⁷, there has been no research done on the water hopping ('skittering') of frogs such as the Indian skipper frog, *Euphlyctis cyanophlyctis*.

Throughout the natural history literature, there are up to 11 species of frogs that are reported to perform skittering locomotion^{1-3,6,8-11,16,19-21,23,25,27}. These frogs vary drastically in size, from the ~1g Northern cricket frog *Acris crepitans* to the largest frog in the world *Conraua goliath*, which can exceed 2 kg as an adult²⁶. With only in-person observations as a source, we have no idea if all of these frogs are actually performing the same locomotor behavior. As the behavior is so quick, we don't even know if the description of skittering as 'bouncing [on the water surface] without sinking¹²' is even accurate. In addition, due to their differing morphology and gait, it is possible that skittering frogs use an entirely different force production mechanism to remain on the water surface compared to the previously studied basilisk lizard or grebe.

The objective of this work is to describe and quantify the skittering locomotion of the Indian skipper frog. Once the kinematics of this

behavior is known, we will be able to physically model the frog's foot-water interactions to estimate the forces the frog produces.

Methods

High-speed recording

Recording took place during the summer of 2016 at the National Centre for Biological Sciences (NCBS) in Bangalore, India. On campus there is a pond that contained a population of around 200 frogs. Several different cameras were used to collect data, included two APX-RS mono Photron high-speed cameras (at 2000 fps), an Edgertronic color high speed camera (at 500 fps), a Fastec TS3 color high-speed camera (at 500 fps), and a Sony 4K video camera (at 30 fps). The two Photron cameras and the Edgertronic were synced together using a function generator so they could be calibrated for 3D reconstruction. The Fastec was used to get zoomed in views of individual jumps during a sequence, and the Sony was used as wide field-of-view in an attempt to capture the entire skittering event.

To record a skittering event, first a target frog was chosen. Frogs were generally chosen such that they were reachable by a telescoping rod, and were fairly isolated (so that multiple frogs would not be triggered at the same time). Frogs were easy to locate as they were usually floating on the water surface. Then, all cameras were moved and focused such that the frog, and an estimate of the frog's future trajectory, were in view. To trigger the frogs into performing their skittering behavior, we slowly extended a telescoping rod under the water such that we disturbed the target frog from below. Cameras would be triggered to save their buffered data once the skittering event was complete.

In order to calculate 3D trajectories from the video data, an extrinsic calibration needed to be performed for every camera setup, so the positions of the cameras could be calculated.

This was done by waving a wand of known length in the field of view.²⁸ To reduce the number of calibrations, we attempted to get as many skittering events as possible for each camera setup. This was possible because during the 15 – 20 minutes required for saving data between trials, frogs would often return to the same floating position they were in previously. Additionally, an intrinsic calibration needed to be recorded for every single lens-camera combination used. This was accomplished by filming a 9x13 symmetric circle grid with 1 cm spacing at various different angles.

Data organization

To determine which skittering sequences were worth digitizing for 3D analysis, all skittering sequences were analyzed for: (1) the total number of jumps in the sequence; (2) how many jumps in the skittering event were recorded in multiple camera views (and therefore able to be projected into 3D); and (3) how many cameras recorded the launch and/or dive of the sequence.

3D trajectory reconstruction

In order to compare different sequences in 3D, it is simplest if all sequences start from the same point – i.e. launching from water. We therefore decided to digitize all sequences in which the frog's launch was visible in at least 2 cameras. In total, 41 sequences fit these parameters, of which 23 contained the full skittering event (launch to dive).

There are several digitization steps required to reconstruct the 3D trajectory of any given sequence. The basic stages of analysis are diagrammed in Figure 1. First of all, for each sequence recorded it is necessary to know not only the position of the cameras relative to each other in 3D space (extrinsics), but also the characteristics of the lenses (intrinsic). To calculate the intrinsic, we recorded 6000 frames of a 9x13 symmetric circle grid moving

and tilting in each camera. Using OpenCV's findCircleGrid⁴, the pixel locations of each dot on the grid were found for at least 1000 frames. These pixel coordinates were then fed into the argus-calibrate script in Argus²² running on the department cluster to calculate the intrinsic matrix components. To calculate the camera extrinsics, we used the wand method developed by Theriault *et. al.*⁸. For each camera setup used to record the skittering frogs, a separate wand calibration was also filmed in which a stick with known length capped by ping pong balls was recorded moving throughout the calibrated volume. The location of both sides of the wand in each camera view for every sequence was tracked semi-automatically using Hedrick's DLTdv7 software¹⁵. These pixel locations, along with the camera intrinsics were then both used to calculate the camera extrinsics using Hedrick's easyWand software²⁸ and sparse-bundle adjustment²⁴. The camera intrinsics and extrinsics together mathematically define where the cameras are in space and how a given 3D point is projected onto each image plane and thus define the 3D calibration of a camera setup.

The next step in calculating the frogs' 3D trajectories is to re-orient the 3D calibrations. When calculating the calibrations using easyWand, the final orientation of the XYZ axes are based on the average projected 3D wand coordinates. However, this is different for each calibration. Instead we want to re-orient the axes such that the Z axis lies on the water surface, so that we can accurately compare the locations of the 3D trajectories. To do this, we took advantage of the lily pads and duck weed that was present on the water surface in most of my recorded sequences. First, we digitized at least 6 points on the water surface (usually the pointed corner of leaves, lily pads, or duckweed) in each camera view for one of the sequences in each camera orientation using DLT. Then, using the initial un-oriented 3D calibration, the 3D coordinates of those

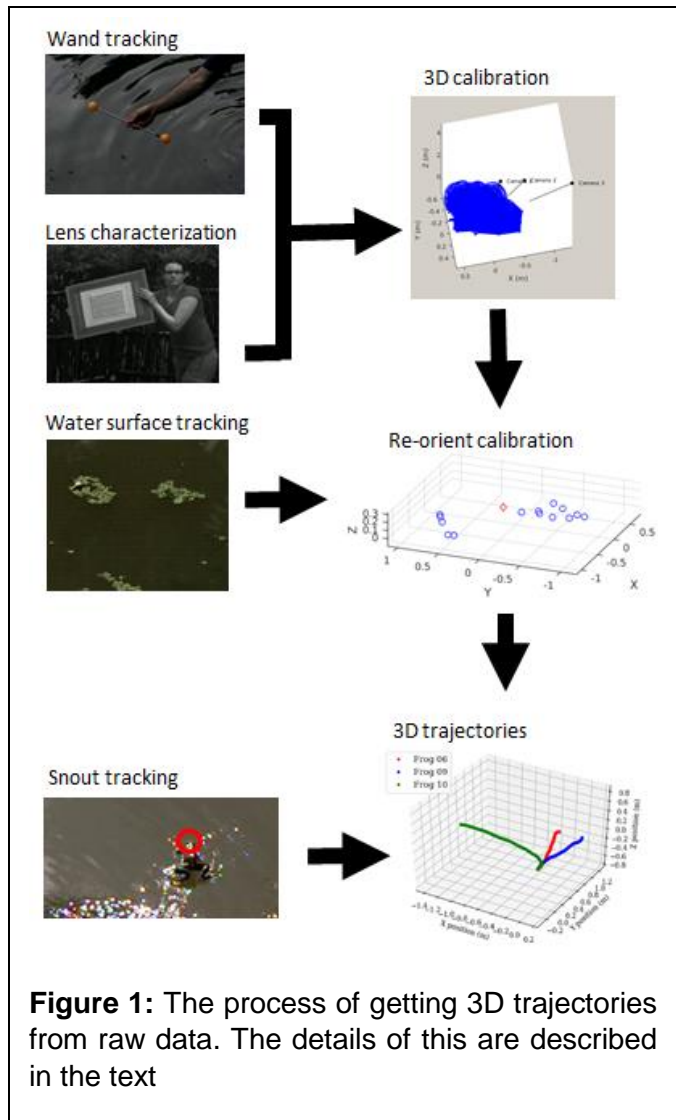


Figure 1: The process of getting 3D trajectories from raw data. The details of this are described in the text

surface points were calculated. A 3D plane was then fit to the surface points. We also digitized a single wand point that was above the water surface and projected it in 3D in order to correctly orient the surface (so the positive Z direction was above the water). Once we had the equation of the water-surface plane, we could calculate the plane's normal vector, and thus the rotation angle and axis required to translate the original 3D calibration to the new, water-surface orientated calibration. Unfortunately, 3 of the 41 sequences picked for 3D reconstruction had insufficient surface debris to re-orient the calibration axes. Therefore, only 39 skittering sequences will

continue to the last step of the 3D reconstruction process.

The final step in calculating the 3D trajectories from the raw video sequences is tracking the frog in every frame of each camera view for a sequence. This was done by hand using DLTdv7. Once the pixel locations of the snout are found in every view, it is very simple to calculate the projected 3D point of each timestep using the 3D calibration for that camera setup and DLTdv7.

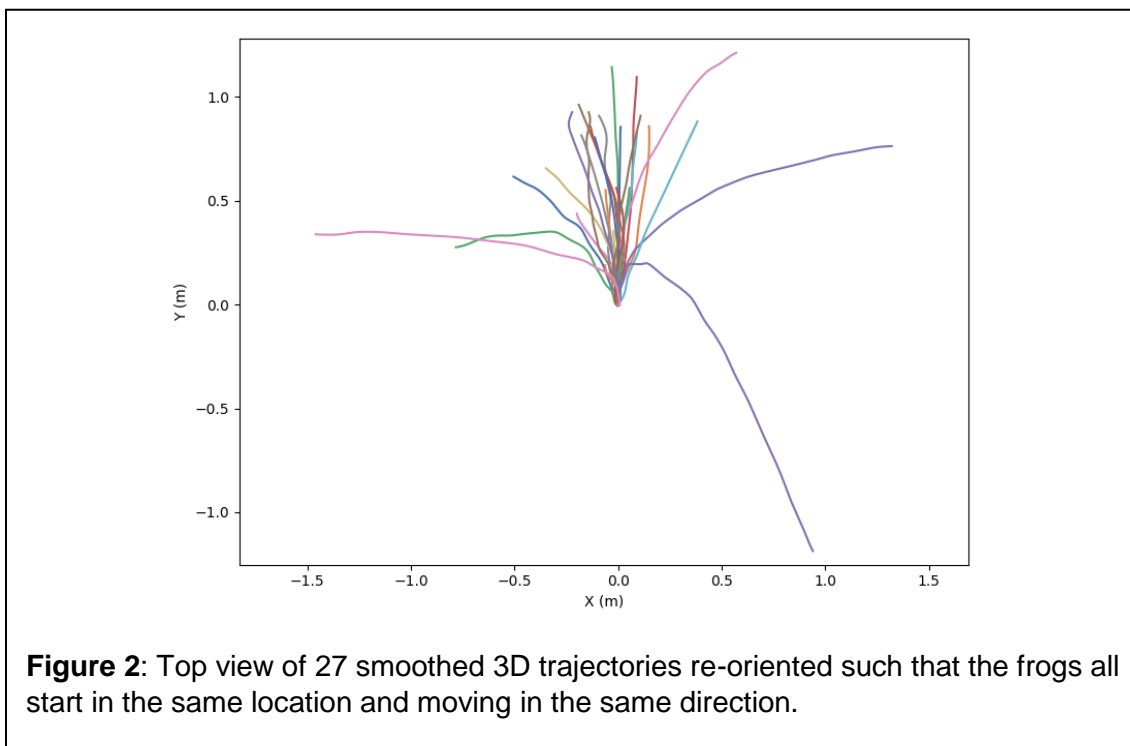
Once each 3D trajectory is calculated, it needs to be smoothed and reoriented. For smoothing, the x, y, and z axes are smoothed individually using a 2nd order butterworth filter applied twice, with the cutoff frequency determined by Winter²⁹. To reorient the trajectories such that they all start in the same location and face the same direction, we used the first 100 timesteps of the frog sequence to calculate an average initial vector of the frog. Then all the 3D points of the trajectory were rotated around the Z axis such that the initial frog vector lies on the Y axis. An example of what the smoothed and re-

oriented 3D trajectories look like when viewing from above can be seen in Figure 2. This reorientation facilitates the comparison of trajectories.

Results

Over the course of a month, we collected over a terabyte of high-speed video data documenting the skittering locomotion of these frogs. This large dataset consists of 109 individual skittering events, 60 of which include full 3D calibrations and 23 of which include planar calibrations. Out of the 109 total sequences recorded, the full skittering event (launch to dive) were captured in 79. Considering only those sequences in which we captured the full skittering event, each frog jumped an average additional 2.95 times after launching from water. The maximum number of times the frog jumped during a skittering event was 9 after the initial jump from water.

While there are 39 sequences deemed appropriate for 3D reconstruction, we have currently only completed tracking the snout on



27. A top view of these sequences can be seen in Figure 2. These trajectories clearly show the maneuverability of the frogs during this skittering behavior. They are capable of turning between successive jumps, something that has not been documented before. In addition, this turning behavior is not seen in the water-running behavior of the grebe or basilisk lizard.

Combining information from the 3D trajectories with how many jumps occurred for each sequence, we can begin to characterize each jump in a skittering event. Ignoring when specifically the frog touches the water surface, we calculated that on average the frog travels 0.25 ± 0.06 m per jump in 0.132 ± 0.24 sec. However, it is possible that the distance traveled and duration of a jump is dependent on where the jump is located in a skittering sequence. For example, the frog may travel less far during the launch jump, as the frog needs to expel itself out of the water in addition to moving forward. To determine this, it is required to know when exactly foot impact occurs during each trajectory. So far, this has been determined by visual inspection in 3 sequences, which can be seen in Figure 3. While this is not yet enough data to do statistical tests, the distance traveled for jump for these 3 frogs was 0.25 ± 0.07 m over 0.123 ± 0.02 sec.

Conclusion

The skittering recordings collected over the summer of 2016 are a very rich video dataset. While there is plenty of qualitative data to be extracted from these videos, such as determining that these frogs can turn during a skittering event, determining how to extract quantitative information from these videos has been a time consuming process. Over this past year, we have finalized the methods for generating the 3D trajectories from the calibrated multi-camera skittering sequences. From the 27 digitized sequences so far, we now know that the frogs are able to travel a

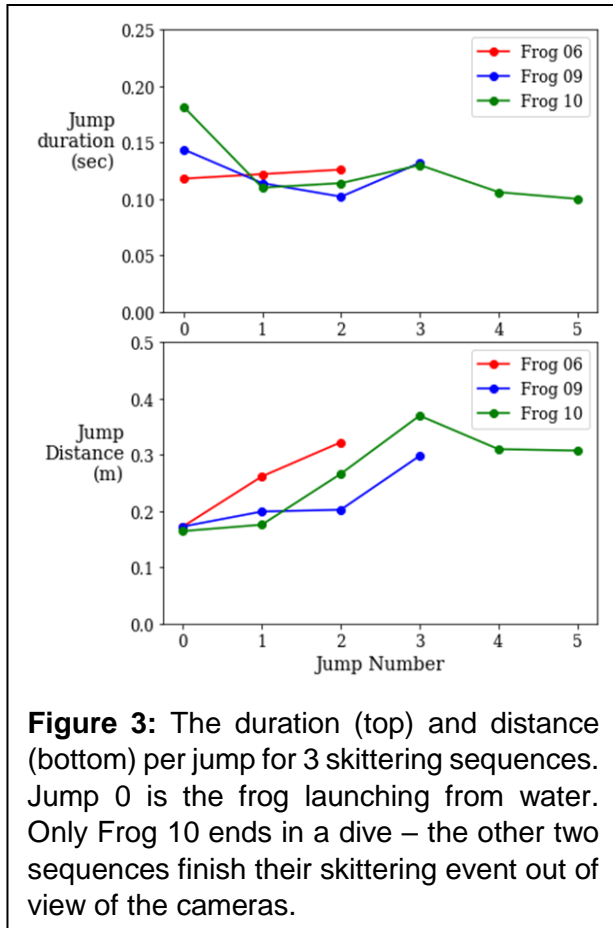


Figure 3: The duration (top) and distance (bottom) per jump for 3 skittering sequences. Jump 0 is the frog launching from water. Only Frog 10 ends in a dive – the other two sequences finish their skittering event out of view of the cameras.

quarter meter per jump, meaning that during a single skittering sequence a frog can travel up to 2 meters, or 40 times their snout-vent length, in a single second (for an 8 jump sequence).

While we are currently only tracking the snout in these videos in order to determine the overall kinematics of skittering behavior, we plan to also track the foot in a subset of videos in order to determine detailed foot kinematics as well. Using the foot velocity, we can make a physical model of the foot impact to directly estimate the force produced by the frog for each jump. This will help explain how the common skittering frog is able to jump on water.

Acknowledgements

This work was supported by the Sigma Xi GIAR program, the APS-IUSSTF India Travel Grant, the Virginia Tech MultiSTEPs IGEP

program, Virginia Tech's Center for Bioinspired Science and Technology and the Virginia Space Grant Consortium Graduate Fellowship.

We would like to thank the Sane lab and NCBS for hosting us (T. Weiss, J. Socha, M. Graham) for a month in Bangalore, India, and Sam Schoedel, Antara Sahay, and Dina Liacopoulos for help in digitizing data.

Publication Plans

We plan to submit the results of this study to the Journal of Experimental Biology by early 2020.

References

1. **Annandale, N.** (1918a). Some Frogs from Streams in the Bombay Presidency. *Rec. Indian Museum* **16**, 121–125.
2. **Babur, Z. and Beveridge, A.** (1922b). The Babur-nama in English. *Trans., Annette Susannah Beveridge*. London: Luzac 2,.
3. **Blair, A. P.** (1950c). Skittering locomotion in *Acris crepitans*. *Copeia* **1950**, 237.
4. **Bradski, G.** (2000d). The OpenCV Library. *Dr. Dobb's J. Softw. Tools*.
5. **Bush, J. W. M. and Hu, D. L.** (2006e). Walking on water: biolocomotion at the interface. *Annu. Rev. Fluid Mech.* **38**, 339–369.
6. **Chabanaud, P.** (1949f). Skittering Locomotion of the African Frog, *Rana occipitalis*. *Copeia* **288**.
7. **Clifton, G. T., Hedrick, T. L. and Biewener, A. A.** (2015g). Western and Clark's grebes use novel strategies for running on water. *J. Exp. Biol.* **218**, 1235–1243.
8. **Cunningham, J. D.** (1964h). Observations on the Ecology of the Canyon Treefrog, *Hyla californiae*. *Herpetologica* **20**, 55–61.
9. **Duellman, W. E. and de Sá, R. O.** (1988i). A new genus and species of South American hylid frog with a highly modified tadpole. *Trop. Zool.* **1**, 117–136.
10. **Dunn, E. and Burden, W.** (1928j). Results of the Douglas Burden Expedition to the Island of Komodo: IV - Frogs from the East Indies. *Am. Museum Novit.*
11. **Flower, S.** (1896k). Notes on a Collection of Reptiles and Batrachians made in the Malay Peninsula in 1895–96; with a List of the Species recorded from that Region. *Proc. Zool. Soc. London*.
12. **Gans, C.** (1976l). The process of skittering in frogs. *Ann. Zool.* **12**, 37–40.
13. **Glasheen, J. W. and McMahon, T. A.** (1996m). A hydrodynamic model of locomotion in the basilisk lizard. *Nature* **380**, 340–341.
14. **Glasheen, J. and McMahon, T.** (1996n). Size-dependence of water-running ability in basilisk lizards (*Basiliscus basiliscus*). *J. Exp. Biol.* **199**, 2611–2618.
15. **Hedrick, T. L.** (2008o). Software techniques for two- and three-dimensional kinematic measurements of biological and biomimetic systems. *Bioinspir. Biomim.* **3**, 034001.
16. **Herrmann, H.-W. and Edwards, T.** (2006p). *Conraua goliath* (Goliath frog). Skittering locomotion. **37**, 202–203.
17. **Hsieh, S. T.** (2003q). Three-dimensional hindlimb kinematics of water running in the plumed basilisk lizard (*Basiliscus plumifrons*). *J. Exp. Biol.* **206**, 4363–4377.
18. **Hsieh, S. T. and Lauder, G. V.** (2004r). Running on water: Three-dimensional force generation by basilisk lizards. *Proc. Natl. Acad. Sci. U. S. A.* **101**, 16784–16788.
19. **Hudson, R. G.** (1952s). Observations on cricketfrog locomotion. *Copeia* **1952**, 185.
20. **Hunter, W. W.** (1908t). *The Imperial Gazetteer of India*. Today and Tomorrow's Printers & Publishers, Faridabad.
21. **Inger, R. F.** (1966u). *Systematics and zoogeography of the Amphibia of Borneo*. Chicago Field Museum of Natural History.
22. **Jackson, B. E., Evangelista, D. J., Ray, D. D. and Hedrick, T. L.** (2016v). 3D for the people: multi-camera motion capture in the field with consumer-grade cameras and open source software. *Biol. Open* **5**, 1334–42.
23. **Janson, H. S.** (1953w). Skittering Locomotion in the Frog *Hyla cinerea cinerea*. *Copeia* **1953**, 62.
24. **Lourakis, M. I. A. and Argyros, A. A.** (2009x). SBA: A Software Package for Generic Sparse Bundle Adjustment. *ACM Trans. Math. Softw.* **36**, 1–30.
25. **Romer, J. D.** (1951y). Surface-locomotion of certain frogs (*Rana*), and the occurrence of *R. taipehensis* Van Denburgh in India. *J. Bombay Nat. Hist. Soc.* **50**, 414–415.
26. **Sabater-Pi, J.** (1985z). Contribution to the Biology of the Giant Frog (*Conraua goliath*, Boulenger). *Amphibia-Reptilia* **6**, 143–153.
27. **Schneider, J. G.** (1799aa). *Historia amphibiorum naturalis et literaria: Fasciculus Primus continens Ranas, Calamitas, Bufones, Salamandras et Hydros in genera et species descriptos notisque suis distinctos, Volume 1*. Frommannus.
28. **Theriault, D. H., Fuller, N. W., Jackson, B. E., Bluhm, E., Evangelista, D., Wu, Z., Betke, M. and Hedrick, T. L.** (2014ab). A protocol and calibration method for accurate multi-camera field videography. *J. Exp. Biol.* **217**, 1843–8.
29. **Winter, D. A.** (2009ac). *Biomechanics and motor control of human movement*. Wiley.